Ferrocenyl catechols: synthesis, oxidation chemistry and anti-proliferative effects on MDA-MB-231 breast cancer cells

Yong Leng Kelvin Tan, Pascal Pigeon, Siden Top, Eric Labbé, Olivier Buriez, Elisabeth A. Hillard, Anne Vessières, Christian Amatore, Weng Kee Leong, Gérard Jaouen

▶ **To cite this version:**

Yong Leng Kelvin Tan, Pascal Pigeon, Siden Top, Eric Labbé, Olivier Buriez, et al.. Ferrocenyl catechols: synthesis, oxidation chemistry and anti-proliferative effects on MDA-MB-231 breast cancer cells. Dalton Transactions, 2012, 41 (25), pp.7537-7549. 10.1039/c2dt30700f . hal-01230385

HAL Id: hal-01230385
https://hal.science/hal-01230385

Submitted on 4 Apr 2024

HAL is a multi-disciplinary open access archive for the deposit and dissemination of scientific research documents, whether they are published or not. The documents may come from teaching and research institutions in France or abroad, or from public or private research centers.

L'archive ouverte pluridisciplinaire **HAL**, est destinée au dépôt et à la diffusion de documents scientifiques de niveau recherche, publiés ou non, émanant des établissements d'enseignement et de recherche français ou étrangers, des laboratoires publics ou privés.

Ferrocenyl catechols: synthesis, oxidation chemistry and anti-proliferative effects on MDA-MB-231 breast cancer cells

Yong Leng Kelvin Tan,[a,b,c] Pascal Pigeon,[a,b] Siden Top,[a,b] Eric Labbé,[d] Olivier Buriez,[d] Elizabeth A. Hillard,[*a,b] Anne Vessières,[a,b] Christian Amatore,[d] Weng Kee Leong[e] and Gérard Jaouen[*a,b]

[a] *ENSCP Chimie Paris Tech, Laboratoire Charles Friedel (LCF), 75005 Paris, France*

[b] *CNRS, UMR 7223, 75005 Paris, France. E-mail: gerard-jaouen@enscp.fr; Tel: +33 (0)1 43 26 95 55; E-mail: hillard@crpp-bordeaux.cnrs.fr; Tel: +33 (0)5 56 84 56 24*

[c] *Hwa Chong Institution, 661 Bukit Timah Road, Singapore 269734, Singapore*

[d] *Ecole Normale Supérieure, Département de Chimie, 24 rue Lhomond, 75231 Paris cedex 05, France*

[e] *Division of Chemistry and Biological Chemistry, School of Physical and Mathematical Sciences, Nanyang Technological University, 21 Nanyang Link, Singapore 637371, Singapore*

Abstract

The synthesis and anti-tumoral properties of a series of compounds possessing a ferrocenyl group tethered to a catechol *via* a conjugated system is presented. On MDA-MB-231 breast cancer cell lines, the catechol compounds display a similar or greater anti-proliferative potency (IC_{50} values ranging from 0.48–1.21 μM) than their corresponding phenolic analogues (0.57–12.7 μM), with the highest activity found for species incorporating the [3]ferrocenophane motif. On the electrochemical timescale, phenolic compounds appear to oxidize to the quinone methide, while catechol moieties form the *o*-quinone by a similar mechanism. Chemical oxidation of selected compounds with Ag_2O confirms this interpretation and demonstrates the probable involvement of such oxidative metabolites in the *in vitro* activity of these species.

1. Introduction

The selective estrogen receptor modulator (SERM) tamoxifen, (*Z*)-2-[4-(1,2-diphenyl-1-butenyl)phenoxy]-*N*,*N*-dimethylethanamine, is the most commonly prescribed drug for treatment of hormone-dependent breast cancer.[1–3] In addition to its use as a chemotherapeutic agent, tamoxifen has also been utilized as a chemopreventive agent for women with a high

risk of contracting breast cancer.[4] The anti-proliferative action of its metabolite hydroxytamoxifen on estrogen receptor positive (ER+) cancers arises due to an anti-estrogenic effect caused by competitive binding to the ER, resulting in the repression of estradiol-mediated DNA transcription.[5,6] However, tamoxifen suffers from limitations as it is ineffective against tumors that do not express the estrogen receptor (ER–). Moreover, the use of tamoxifen has been associated with an increase in the risk of uterine and endometrial cancer.[7,8] Tamoxifen and hydroxytamoxifen can be further metabolized to the catechol 3,4-dihydroxytamoxifen.[9] The latter catechol undergoes oxidation by a variety of oxidative enzymes and metal ions to give an *o*-quinone (OQ) which can cause oxidative damage to cellular DNA through redox cycling with reactive oxygen species such as semi-quinone radicals.[10] The OQ is also electrophilic in nature and can cause cell damage *via* alkylation of amino acid residues on proteins and covalent binding to DNA.[11]

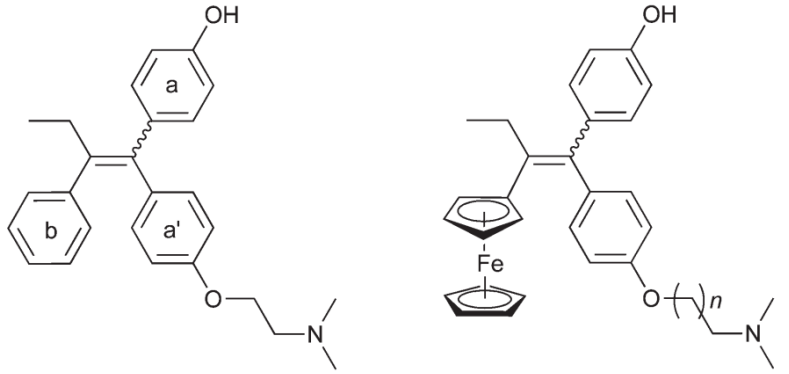

Hydroxytamoxifen

Hydroxyferrocifens
n = 1, 2, 3, 4, 7

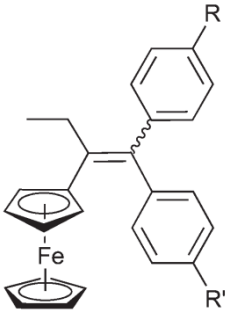

Ferrocenyl phenols
1a R = R' = OH
2a R = OH, R' = H

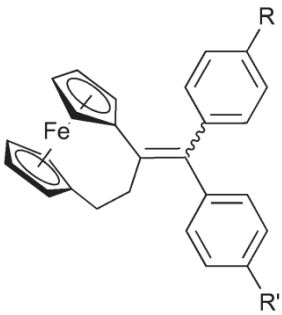

Cyclic ferrocenyl phenols
1b R = R' = OH
2b R = OH, R' = H

Chart 1 The SERM hydroxytamoxifen and its ferrocenyl derivatives.

A major research focus of our group is the investigation of the biological activity of organometallic moieties tethered to SERMS. We have previously synthesized a series of compounds which we have termed "hydroxyferrocifens", by covalently grafting ferrocene onto the hydroxytamoxifen backbone. By modification of several structural aspects, these hydroxyferrocifens have been further developed into the ferrocene phenols, **1a** and **2a** (Chart 1). Some of these organometallic biovectors demonstrate a high *in vitro* anti-proliferative activity, *via* the combination of anti-estrogenicity and cytotoxicity on hormone-dependent (MCF-7) breast cancer cell lines as well as a cytotoxic effect on hormone-independent (MDA-MB-231) breast cancer cells.[12–15] The strong *in vitro* activity correlates with the presence of a ferrocene group, a *p*-phenol, and a π-system linking these two functionalities.[14,16–19] We have posited that the activation pathway involves the oxidation of the phenol moiety *via* the ferrocene group to generate an active quinone methide (QM) species, and have shown that these QMs were indeed formed in the presence of rat liver microsomes as well as during chemical oxidation with silver oxide.[20,21] More recently, we have synthesized cyclic ferrocenyl compounds based on the [3]ferrocenophane motif, **1b** and **2b**, and found them to be considerably more potent than their non-cyclic analogues **1a** and **2a**.[22–24] As part of our ongoing investigations into the biological activity of the above-mentioned compounds, we were interested in examining the *in vitro* effects of their catechol analogues. In this article, we present the synthesis, electrochemical and chemical oxidation studies for a series of catechol ferrocene and [3]ferrocenophane compounds. The results of biological tests to evaluate the antiproliferative effects of these catechol compounds on hormone-independent breast cancer cell lines, as compared to their phenolic analogues, will also be reported.

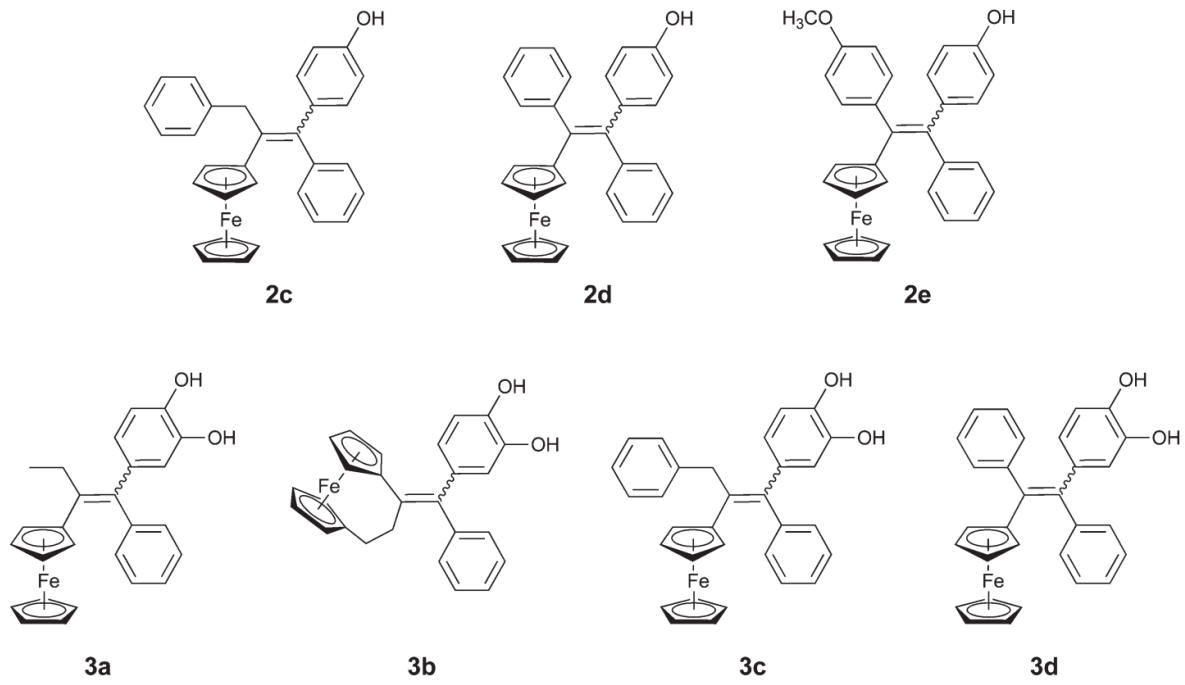

Chart 2 New ferrocenyl tamoxifen derivatives studied in this report.

Results and discussion

2.1 Synthesis and characterization

Previous studies have shown that the diphenols **1a** and **1b** are more cytotoxic than their monophenol analogues **2a** and **2b**. We were curious to know if the presence of two hydroxyl groups on the same phenyl ring would similarly enhance the activity of the ferrocene tamoxifen derivatives. To approach this question, we naturally began by synthesizing the catechol analogues of **2a** and **2b** (compounds **3a** and **3b**, Chart 2). The phenol (**2c**) and catechol (**3c**) compounds where a phenyl group replaces the CH_3 group were also prepared with the assumption that the phenyl substituent could favor QM formation by extending the conjugated system and thus stabilizing the oxidation product. As compounds **3a**, **3b** and **3c** could theoretically be metabolized to either a QM or an OQ, we also prepared the phenol compound **2d** and the catechol **3d** where the lack of a labile proton β to the ferrocene group would prevent extended QM formation.

A McMurry cross-coupling between 4-hydroxybenzophenone or 3,4-dihydroxybenzophenone with [3]ferrocenophan-1-one or the appropriate ferrocenyl ketone provided the general synthetic route to all of the ferrocenyl phenol and catechol compounds shown in Chart 2, which were obtained in moderate to good yields. For example, a Friedel–Crafts reaction of

propionyl chloride with ferrocene afforded ethyl ferrocenyl ketone, which was further combined with 3,4-hydroxybenzophenone to afford the dark red compound **3a** in 65% yield (Scheme 1).[25] Efforts to obtain the compound with vicinal phenol groups (**2f**) were unsuccessful. The mixture obtained from the McMurry coupling reaction between 4-hydroxyphenyl ferrocenyl ketone and 4-hydroxybenzophenone was found to decompose rapidly during the process of chromatographic separation on a silica gel column, and attempts to deprotect the phenol in **2e** by removing the methyl group using boron tribromide at ambient temperature also resulted in decomposition of the reaction mixture. An endeavor to obtain the catechol analogue of **2f**, *viz*. **3f**, by reacting 4-hydroxyphenyl ferrocenyl ketone and 3,4-dihydroxybenzophenone also failed to give the expected product. The reaction of **3a** with an excess of acetyl chloride at ambient temperature afforded the diacetoxy derivative **4**, as well as the monoacetoxy derivatives **5** and **6**; the latter two isomeric compounds could not be separated by chromatography or on semi-preparative HPLC.

All the novel compounds were characterized spectroscopically and analytically. Molecular ion peaks are present in all their respective mass spectra; for the acetylated derivatives **4**–**6**, peaks corresponding to loss of $CH_3CO^{\cdot}$ fragments are displayed as well. Consistent with previous observations, the McMurry reaction resulted in both the *Z*- and *E*-isomers of the tetrasubstituted olefins. We were unable to separate the geometric isomers of each compound by chromatography, and the presence of both isomers was observed in the solution ^{1}H NMR spectra. After fractional crystallization, compounds *E*-**2c**, *Z*-**2d**, *Z*-**2e** and *Z*-**4** were studied by single-crystal X-ray diffraction methods, and the ORTEP diagrams of *E*-**2c**, *Z*-**2e** and *Z*-**4** are illustrated in Fig. 1 (*Z*-**2d** omitted for brevity). A common atomic numbering scheme, together with selected bond parameters for all four compounds are collected in Table 1. For each molecule, there is a narrowing of the bond angle between the two substituents connected to the same carbon atom of the double bond, presumably to minimize steric interaction with their *cis*-disposed neighbours. While the planarity of the ethylenic skeleton is mainly retained, the phenyl moieties in each molecule are tilted with respect to the olefinic plane, ranging from 44.5(2)° in *Z*-**2e** to 71.5(2)° in *Z*-**2d**. The cyclopentadienyl ring attached to the double bond also displays deviation from the latter plane, with observed twist angles between 13.6(2)° in *Z*-**2d** to 31.5(2)° in *Z*-**4**.

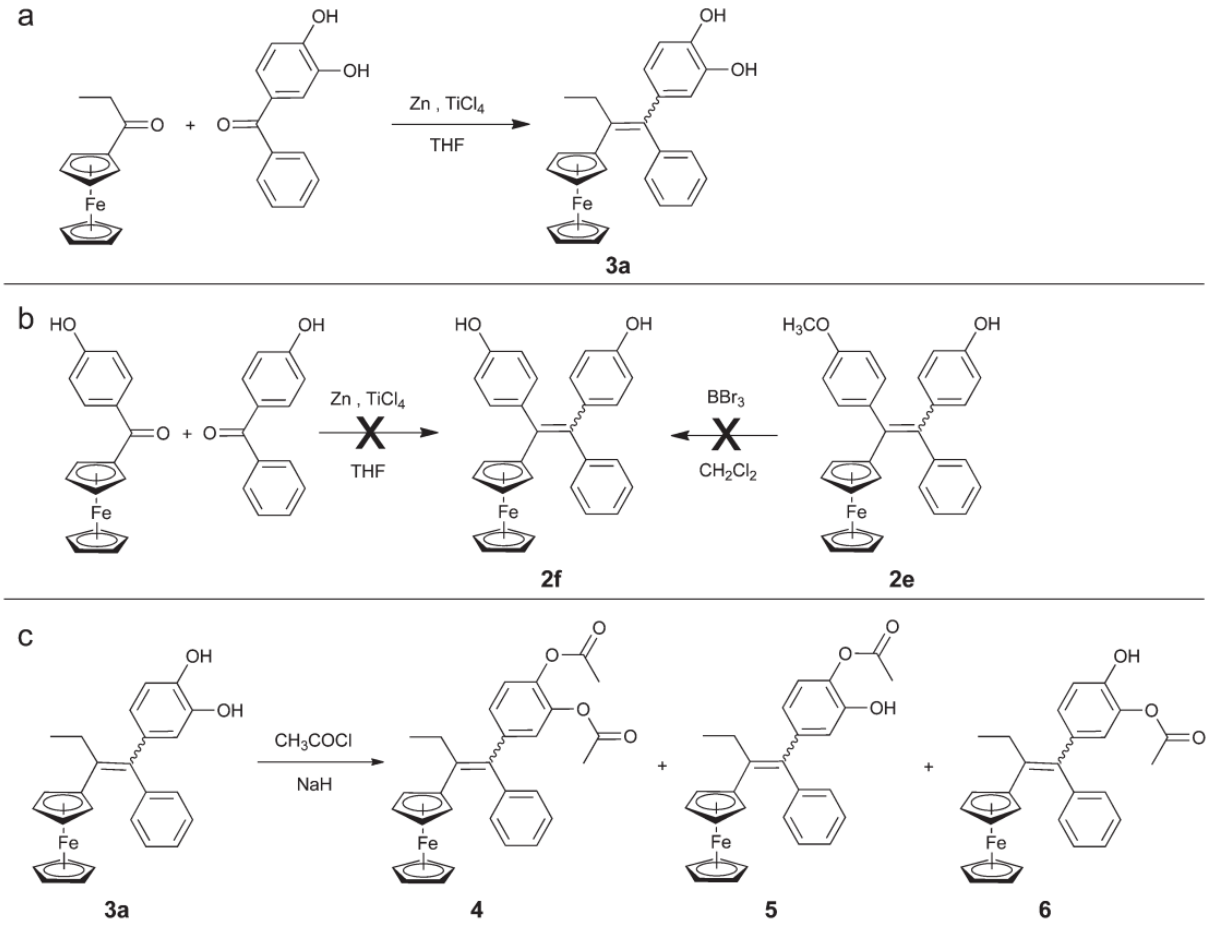

Scheme 1 (a) Synthesis of **3a** by McMurry cross coupling (similar procedure used for synthesis of **2c–e** and **3a–d**) and; (b) Neither McMurry cross coupling nor deacetylation yielded the desired compound **2f**; (c) Acetylation of compound **3a** yielded **4**, **5** and **6**.

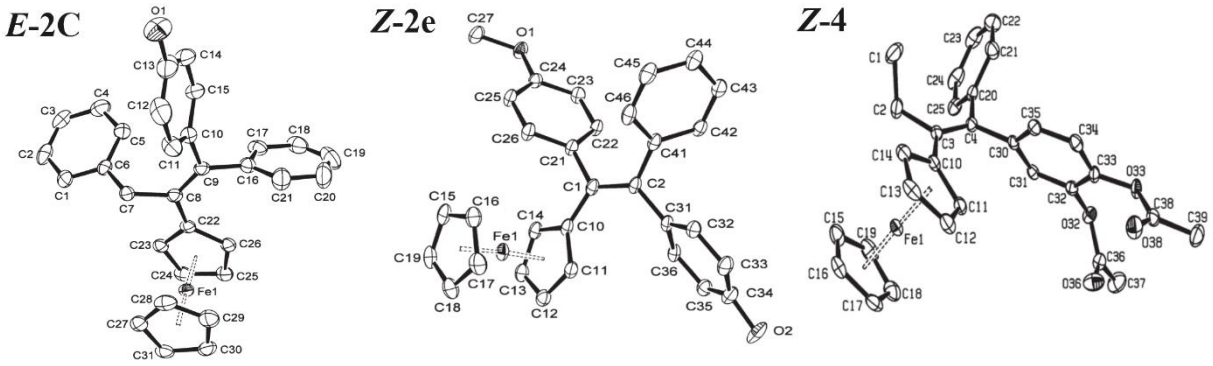

Fig. 1 ORTEP diagrams (50% probability thermal ellipsoids, organic hydrogen atoms omitted) for *E*-**2c**, *Z*-**2e** and *Z*-**4**.

CCDC 829115–829118

Table 1 Common atomic numbering scheme and selected bond parameters for *E*-**2c**, *Z*-**2d**, *Z*-**2e** and *Z*-**4**

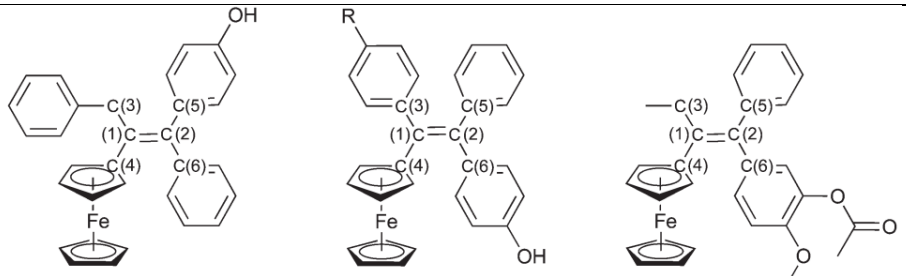

***E*-2c** **Z-2d** R = H **Z-2e** R = OCH_3 ***Z*-4**

	E-**2c**	*Z*-**2d**	*Z*-**2e**	*Z*-**4**
Bond lengths (Å)				
C1–C2	1.343(5)	1.349(4)	1.360(3)	1.345(3)
C1–C3	1.528(4)	1.503(4)	1.499(3)	1.526(3)
C1–C4	1.481(4)	1.482(4)	1.473(3)	1.475(3)
C2–C5	1.496(5)	1.494(4)	1.490(3)	1.499(3)
C2–C6	1.498(4)	1.500(3)	1.489(3)	1.495(3)
Bond angles (°)				
C3–C1–C4	114.6(3)	115.3(2)	114.95(18)	115.35(16)
C5–C2–C6	113.0(3)	114.1(2)	114.66(17)	112.98(16)
C3–C1–C2–C5	4.3(3)	10.0(2)	19.5(2)	2.5(2)
C4–C1–C2–C6	6.1(3)	2.5(2)	11.4(2)	0.1(2)
C3–C1–C2–C6	−170.3(2)	−171.4(2)	−159.5(2)	−173.3(2)

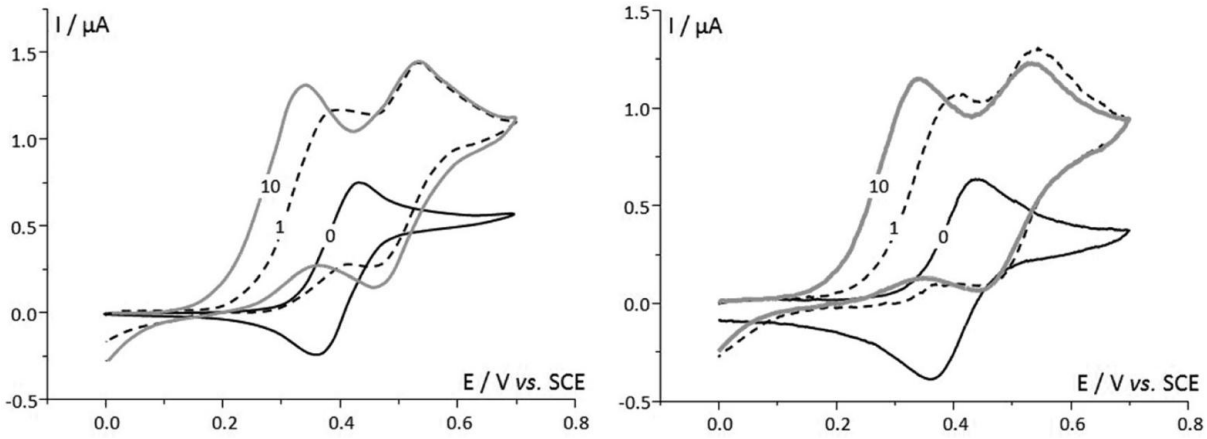

Fig. 2 Cyclic voltammograms of **3a** (left) and **3c** (right) 1 mM in acetonitrile + Bu_4NBF_4 (100 mM). Platinum electrode (Ø = 0.5 mm), scan rate 0.2 V s^{-1}. CVs recorded in the absence (black solid line) and in the presence of 1 molar equivalent (black dashed line) and 10 molar equivalents (grey solid line) of imidazole.

2.2 Electrochemistry

We previously hypothesized that the anti-proliferative effects of several ferrocenyl phenols, such as **1a** and **2a**, are associated with their *in situ* oxidation to QM species.[20,21,26] The ferrocene moiety seems to act as an intramolecular oxidant *via* a proton-coupled electron transfer process which can be observed on the electrochemical timescale. In order for QM formation to occur *via* this process, the molecules must possess an appropriate geometry; namely the presence of a ferrocene group conjugated to a *p*-phenol, with a labile proton β to the ferrocene group. For example, **2c** differs from **2a** only by the replacement of the ethyl group by a benzyl moiety. Therefore, all of the requirements for ferrocene-mediated QM formation are met, and, indeed, the cyclic voltammetry in wet dichloromethane in the presence and absence of added 2,6-dimethylpyridine is similar to what was previously observed for **2a** in methanol and pyridine (ESI).* On the other hand, compounds **2d**, **2e** and **3d** lack such a labile proton. While neither **2d** nor **2e** show reactivity with the added base, **3d** displays an electrochemical signature suggestive of proton-coupled electron transfer. While a QM structure is not apparently feasible for **3d**, it should be noted that the *o*-quinone is also a possible two-electron oxidation product. Catechol compounds **3a–c**, possessing a labile proton β to the ferrocene group, can theoretically form either the QM or the *o*-quinone after a two-electron oxidation. The cyclic voltammograms for **3a–c** more closely resemble that of **3d** than **2a**, suggesting that the *o*-quinone may be formed on the electrochemical timescale (ESI).

*Although our earliest studies attempted to model the cellular environment using methanol (the lipophilic ferrocifens being essentially insoluble in water), we quickly realized that other organic solvents have certain practical advantages, and are not less appropriate than methanol when considering that these compounds are probably activated by a base found not in the cytoplasm but in a biomolecule. It should be mentioned that no solvent dependence has been observed in the electrochemical studies of ferrocifen derivatives.

The electrochemical behavior of **3a** and **3c** was further explored by cyclic voltammetry in acetonitrile (ESI). The voltammograms obtained in the absence and presence of imidazole are presented in Fig. 2. In the absence of imidazole, one can observe the one-electron oxidation of **3a** at a peak potential value of 0.42 V/SCE. This electrochemical step is ascribed to the reversible oxidation of the ferrocene group (Fc) to ferricenium (Fc^+), in agreement with the behavior of analogous ferrocenyl tamoxifen derivatives.[20] In the presence of imidazole, two oxidation steps are observed; a nearly 2-electron irreversible oxidation peak appears, the potential of which shifts towards less positive values as the imidazole concentration increases. Another peak located at 0.52 V/SCE features a 1-electron reversible oxidation process, its potential being independent of imidazole concentration. The CVs obtained with **3c** (right panel) under the same conditions are akin to those for **3a** (left panel). We recently carried out

a study devoted to the determination of the oxidation mechanism of a model ferrocene phenol, which showed a very similar base-dependent electrochemical behavior.[27] Parallel EPR and electrochemical monitoring of electrolyses established that the first 2-electron oxidation process corresponds to the passage from a phenol to a QM, followed by the 1-electron oxidation of the ferrocene group of the latter species. The base (imidazole) triggers an oxidation sequence made possible by the increased acidity of the phenol proton of the ferricenium cation generated upon oxidation of the starting ferrocene phenol compound. In the present study, an OQ could be generated instead of a QM, as featured in Scheme 2. In the absence of imidazole, one only observes the reversible one-electron oxidation of **3a** and **3c** (step (1)). In the presence of excess imidazole, a 2-electron oxidation sequence occurs according to steps (1) + (2) + (3). At low scan rates (Fig. 2), the potential dependence of this bielectronic wave with excess imidazole features the thermodynamically favored passage from a monoelectronic Fc oxidation to a proton-coupled bielectronic oxidation of the catechol. Note that the deprotonations are most likely concerted to the electron transfers, at least within the time range explored. The following one-electron process corresponds to the reversible oxidation of the orthoquinone into its ferricenium analogue (step (4)). Moreover, the (1) + (2) + (3) sequence is fast enough to be observed within the same scan in the presence of imidazole.

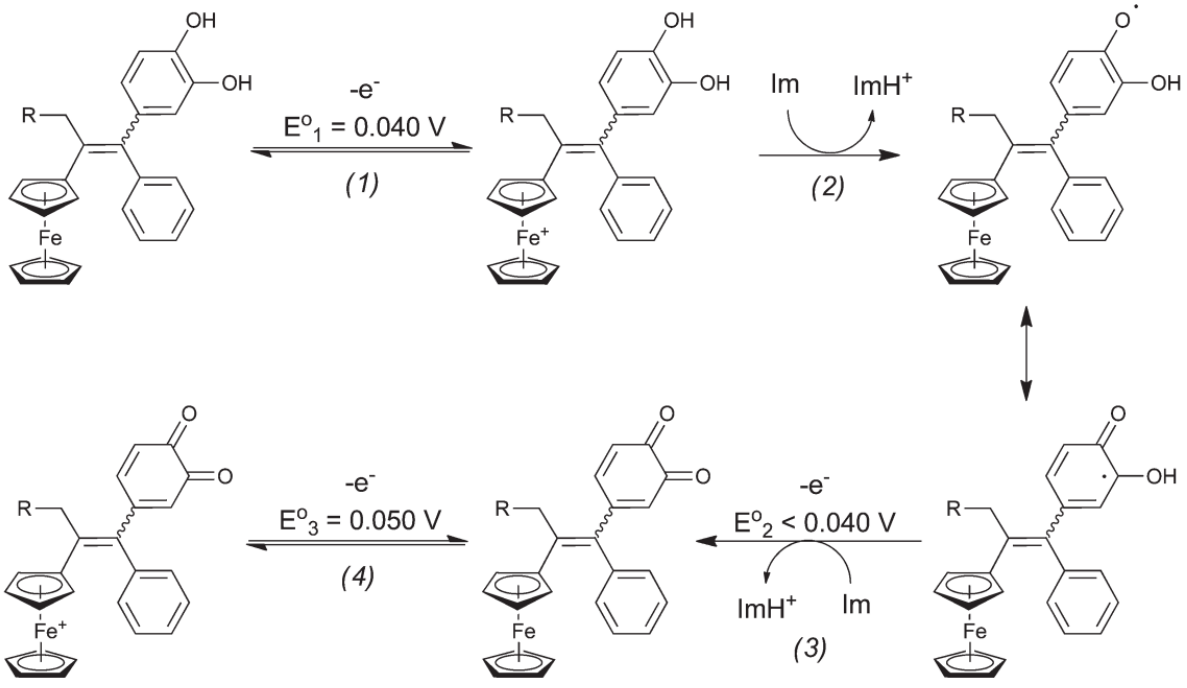

Scheme 2 Base-promoted oxidation sequence of catechols **3a** and **3c**.

In order to confirm this oxidation mechanism, we performed preparative electrolyses of catechols **3a** and **3c** in the presence of imidazole at 0.48 V/SCE, *i.e.* the potential value corresponding to the diffusion tail of the first bielectronic wave and to the foot of the second monoelectronic wave. The concentration of the species was monitored by cyclic voltammetry, as reported in Fig. 3. For both compounds, the complete electrolysis at 0.48 V/SCE in the presence of imidazole corresponds to a total charge of *ca.* 2 Faraday mol^{-1}. Curves c and c′, recorded after the electrolyses, no longer display the original 2-electron oxidation wave (as seen in curves b and b′ recorded before the electrolyses) and the CVs only show the reversible one-electron oxidation ascribed to the OQ. Finally, the bielectronic nature of the first wave is quantitatively confirmed at the time scale of preparative electrolyses.

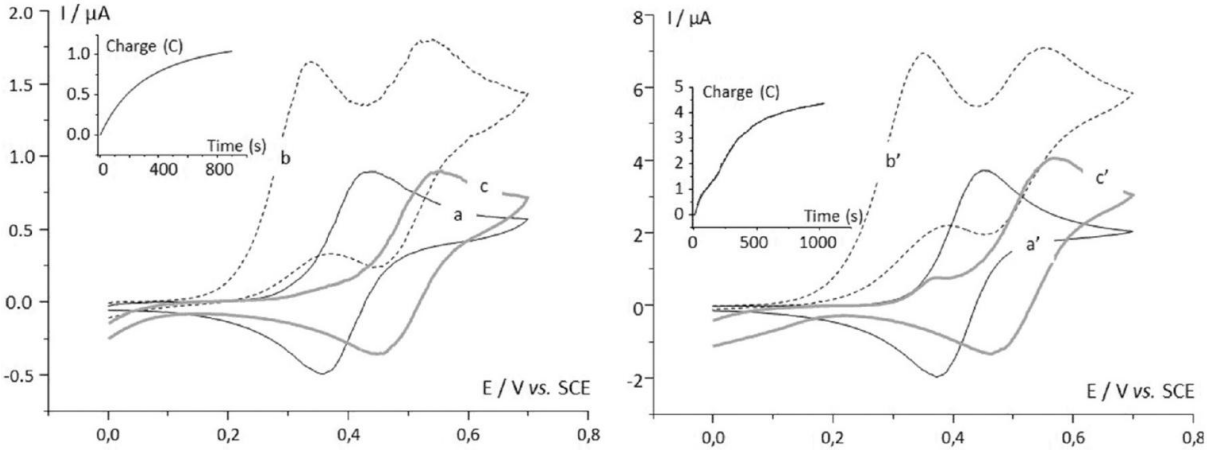

Fig. 3 Cyclic voltammograms of acetonitrile + Bu_4NBF_4 (200 mM) solutions (platinum electrode Ø = 0.5 mm, scan rate 0.1 V s^{-1}) at various electrolysis stages. Left panel: Compound **3a** 1.2 mM (curve a); Compound **3a** 1.2 mM + imidazole 15 mM (curve b); and Compound **3a** 1.2 mM + imidazole 15 mM + 1.95 Faraday mol^{-1} electrolysis at 0.48 V/SCE (curve c) Right panel: Compound **3c** 6 mM (curve a′); Compound **3c** 6 mM + imidazole 75mM (curve b′); and Compound **3c** 6 mM + imidazole 75 mM + 1.8 Faraday mol^{-1} electrolysis at 0.48 V/SCE (curve c′). Insets = evolution of the charge vs. time during electrolysis.

The electrochemical oxidation of catechols **3a** and **3c** is dramatically affected by the presence of imidazole. In the absence of this base, both catechols only oxidize according to a reversible one-electron process centered on the ferrocene group. In the presence of imidazole, the CVs display two distinct processes, the first one corresponding to the bielectronic oxidation of the catechol to the OQ, the second one being the ferrocene-centered one-electron reversible oxidation of the OQ formed at the first wave. The oxidation sequence, although leading to

OQs, displays kinetic and thermodynamic features very similar to those encountered in the electrochemical oxidation of ferrocene phenols to QMs.

2.3 Chemical oxidation

The reaction of **2d** and **2e**, lacking a labile proton β to the ferrocenyl group, with silver oxide in acetone afforded only unreacted starting compounds, as expected. Interestingly, Ag_2O does not directly oxidize the ferrocene group to ferricenium, and therefore the previously reported transformation of compounds such as **1a** to the quinone methide using Ag_2O probably does not involve the intramolecular electron transfer process observed in the electrochemical experiments. Nonetheless, the use of Ag_2O allows us to determine whether or not a QM or OQ can ultimately be formed and to isolate such oxidation products.

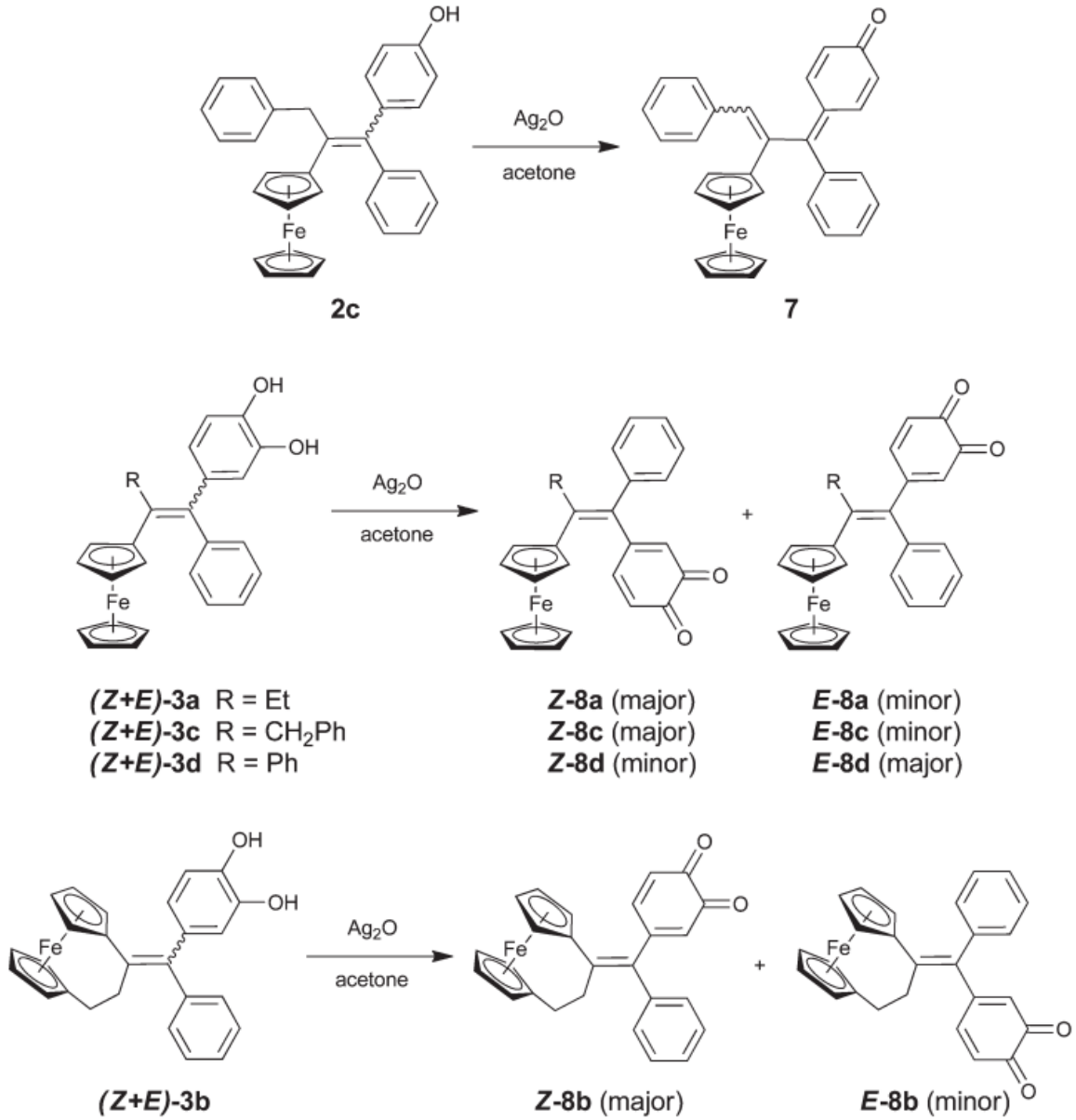

Scheme 3 Chemical oxidation of compounds **2c** and **3a–d**.

In contrast to the unreactive **2d** and **2e**, chemical oxidation of **2c** resulted in the formation of the QM **7** (Scheme 3), in accord with the electrochemical observations. Compound **7** was identified by the presence of a carbonyl stretch at 1709 cm^{-1} in the infrared spectrum, as well as a molecular ion peak (*m/z* 468) indicating the loss of two hydrogen atoms from the parent compound **2c** (*m/z* 470). For the ^{13}C NMR spectrum of **7**, the resonance at δ 187.2 ppm is ascribable to the presence of a C=O group. In the ^{1}H NMR spectrum, the multiplet signals in the δ 6.24–7.25 ppm range, which integrate to a total of five hydrogen atoms, are assigned to the protons of the quinone ring as well as the single vinylic proton, while the more deshielded

multiplets in the δ 7.41–7.67 ppm range, which integrate to a total of ten protons, can be attributed to the phenyl rings.

The catechol compounds **3a–d** reacted with silver oxide in acetone to give the corresponding *o*-quinones **8a–d**, as suggested by the electrochemical experiments. While quantitative formation of **8b–d** was observed after twenty minutes, the complete conversion of **3a** to **8a** took one hour. At twenty minutes, the oxidation of **3a** yielded a mixture of **8a**, the QM as well as starting material; the ratio of **8a** to the latter two compounds was approximately 9 : 1. Carbonyl stretches at 1650 cm^{-1} are displayed in the infrared spectra of the OQs. Singlet signals are also present in the δ 180 ppm region of the ^{13}C NMR spectra. The ^{1}H NMR spectra of **8a–d** indicate that the protons of the *o*-quinone ring are shielded as compared to the protons of the catechol ring in **3a–d**. In addition, the proton signals attributable to the cyclopentadienyl rings of the *o*-quinone compounds are deshielded relative to their catechol precursors (Table 2). Assuming that the proximity of the *o*-quinone ring would result in a greater impact on the chemical shift of the protons of the cyclopentadienyl rings of the *Z*-isomer than that of the *E*-isomer, analysis of the chemical shifts in the proton NMR spectra suggests that the major isomers of **8a**, **8b** and **8c** have the *Z* configuration while **8d** has the *E* configuration.

Table 2 NMR assignments for **3a–d** and **8a–d** (cyclopentadienyl rings, in CD_3COCD_3)

	δH (ppm)			δH (ppm)	
Compound	C_5H_4	C_5H_5	Compound	C_5H_4	C_5H_5
(*Z*+*E*)-**3a**	4.04 (2H), 3.84 (2H)[a]	4.11 (5H)[a]	*Z*-**8a**[b]	4.58 (2H), 4.53 (2H)[a]	4.28 (5H)[a]
	4.07 (2H), 3.96 (2H)	4.12 (5H)			
			E-**8a**[b]	4.18 (2H), 3.91 (2H)	4.17 (5H)
(*Z*+*E*)-**3b**	4.26 (2H), 4.04 (2H)[a]		*Z*-**8b**[b]	4.49 (2H), 4.46 (2H)[a]	—
	4.00 (2H), 3.94 (2H)[a]			4.25 (2H), 3.98 (2H)[a]	
	4.24 (2H), 4.02 (2H),		*E*-**8b**[b]	4.37 (2H), 4.07 (2H),	—

	3.97 (2H), 3.96 (2H)			4.04 (2H), 3.94 (2H)	
(*Z*+*E*)-**3c**	3.99 (2H), 3.82 (2H)[a]	4.13 (5H)[a]	*Z*-**8c**[b]	4.45 (4H)[a]	4.35 (5H)[a]
	3.94 (2H), 3.69 (2H)	4.16 (5H)			
			E-**8c**[b]	4.15 (2H), 3.88 (2H)	4.24 (5H)
(*Z*+*E*)-**3d**	4.06 (2H), 3.54 (2H)[a]	4.15 (5H)[a]	*Z*-**8d**[b]	4.48 (2H), 4.30 (2H)	4.28 (5H)
	4.01 (2H), 3.39 (2H)	4.12 (5H)			
			E-**8d**[b]	4.24 (2H), 3.51 (2H)[a]	4.25 (5H)[a]

[a] Peaks belonging to major isomer. [b] Assignments of isomers performed based on δ (see text).

Table 3 Cytotoxicity of **1a**, **2a–e**, **3a–d** and **4** on MDA-MB-231 breast cancer cell lines

Compound	Phenol or catechol	IC_{50} (μM)[a]	Presumed metabolite[b]
(*Z*+*E*)-**1a**	2 phenols	0.29 ± 0.07	QM
(*Z*+*E*)-**2a**	1 phenol	1.80 ± 0.03	QM
(*Z*+*E*)-**2b**	1 phenol	0.57 ± 0.03	QM
(*Z*+*E*)-**2c**	1 phenol	5.3 ± 0.9	QM
(*Z*+*E*)-**2d**	1 phenol	9.0 ± 1.0	None
(*Z*+*E*)-**2e**	1 phenol	12.7 ± 1.6	None
(*Z*+*E*)-**3a**	Catechol	1.10 ± 0.07	OQ
(*Z*+*E*)-**3b**	Catechol	0.48 ± 0.04	OQ
(*Z*+*E*)-**3c**	Catechol	1.21 ± 0.07	OQ
(*Z*+*E*)-**3d**	Catechol	2.4 ± 0.2	OQ
(*Z*+*E*)-**4**	Protected catechol	15.1 ± 1.5	None

[a] Mean of two experiments ± range. [b] As determined by electrochemical or chemical oxidation.

2.4 Effect on growth of hormone-independent breast cancer cells MDA-MB-231

Compounds **2**, **3** and **4** were screened for their anti-proliferative effects on the MDA-MB-231 breast cancer cell line, and the results are recorded in Table 3. This line is hormone

independent and does not express the estrogen receptor, hence on these cell lines the observed anti-proliferative effect can be attributed only to a cytotoxic effect potentially induced by the ferrocenyl unit. Compounds **2d** and **2e**, which remained inert to chemical oxidation and cannot undergo ferrocene-mediated QM formation, were markedly less active on the cells as compared to **2a–c** which were able to be oxidized to quinone species; this provides further support for our proposal that oxidation to QM moieties could be the key to the anti-proliferative effect displayed by these ferrocenyl compounds. Along these same lines, the lower activity of **2c** can be attributed to the extended conjugated system that would be expected to stabilize the QM towards nucleophilic attack in the cell. It should be mentioned that the IC_{50} values of **1a** (0.6 μM)[28] and **2a** (1.13 μM)[22] have been previously determined, using a 24-well plate after five days. The currently reported values, obtained using a 96-well plate after 72 h vary somewhat, but are on the same order of magnitude.

Interestingly, although previous work showed that **1a** and its acetylated form show equal activity against MDA-MB-231 cells,[29] compound **4**, the acetylated derivative of **3a**, is not active. The steric bulk of two acetyl groups *ortho* to one another may prevent the protecting groups from being hydrolyzed in the cell.

The ferrocenyl catechols have similar (**3a** and **3b**) or stronger (**3c** and **3d**) anti-proliferative potency to their corresponding phenolic analogues **2a–d**. This is in contrast to previous reports that 3,4-dihydroxytamoxifen and 3,4-dihydroxytoremifen had lower biological activity than 4-hydroxytamoxifen and 4-hydroxitoremifen, respectively, leading the authors to conclude that the metabolism of tamoxifen and toremifen to their catechols might play a minor role in the cytotoxicity of the purely organic molecules.[10,30] The addition of ferrocene thus reverses the trend such that the catechols show similar activity towards the cancer cells as the phenolic compounds. Compound **3b**, with the [3]ferrocenophane structure, displays the highest anti-proliferative effect amongst the catechol complexes. This is consistent with our previous observations on these types of molecules, and the enhanced efficacy of the compounds bearing the [3]ferrocenophane motif may be attributed to the narrower HOMO–LUMO gap present in the oxidized form of the [3]ferrocenophane moieties, giving rise to more reactive species.[31] Compounds **2d**, **2e** and **4** cannot form either the QM or the OQ *via* ferrocene-mediated oxidation due to their geometry. These compounds have the lowest activity of the series, suggesting that ferrocene is an important mediator of the oxidation process. We have postulated that ferrocenyl group acts as a redox antenna that triggers the oxidation of the phenol function in conjugated systems. The present results support this

hypothesis, and we furthermore see that the ferrocenyl group also plays an important role in the oxidation of the catechol derivatives. The molecule can transform into a quinone methide or an orthoquinone, depending on the location of the most acidic proton, and the ease of the phenol oxidation by delocalization of the radical is the key to the antiproliferative activity of compounds.

Experimental

3.1 General procedures

All reactions and manipulations were carried out under an argon atmosphere using standard Schlenk techniques. THF was distilled over sodium–benzophenone prior to use. Column chromatography was performed on silica gel 60 M. Semi-preparative HPLC separations were performed on a Shimadzu instrument with a Kromasil C18 column (length of 25 cm, diameter of 2 cm, particle sizes of 10 μm) using acetonitrile as eluent. IR spectra were obtained on a BOMEM Michelson 100 spectrometer. ^{1}H and ^{13}C NMR spectra were acquired on a Bruker 300 MHz spectrometer. The solvent used was deuterated chloroform unless otherwise stated. Mass spectrometry was carried out at the Service de Spectrométrie de Masse at ENSCP, Paris. High resolution mass spectra (HRMS) were obtained by the Groupe de Spectroscopie de Masse of the Laboratoire de Structure et Fonction de Molécules Bioactives at the University of Pierre et Marie Curie, Paris. Microanalyses and biochemical experiments were performed, respectively, by the Service de Microanalyse and IMAGIF at the ICSN (Gif sur Yvette, France).

Benzyl ferrocenyl ketone, phenyl ferrocenyl ketone, 4-methoxyphenyl ferrocenyl ketone, ethyl ferrocenyl ketone and [3]ferrocenophan-1-one were synthesized according to procedures found in the literature.[32–34] All other reagents were from commercial sources and used as supplied.

3.2 Reactions of ferrocenyl ketones with benzophenones

In a typical reaction, $TiCl_4$ was added dropwise to a suspension of zinc powder in 80 mL of THF and the mixture was heated at reflux for 2 h. A second solution was prepared by dissolving the ferrocenyl ketone and benzophenone in THF (30 mL). The latter solution was added dropwise to the first solution and the resulting mixture was heated at reflux. After cooling to room temperature, the mixture was stirred with water and CH_2Cl_2. The mixture was acidified with dilute HCl until the dark color disappeared and was decanted. The aqueous

layer was extracted with CH_2Cl_2 and the combination of organic layers dried on $MgSO_4$. This was followed by filtering the mixture and removing the solvent under reduced pressure. Chromatographic separation on a silica gel column with hexane–CH_2Cl_2 as the eluent afforded compounds **2c–e** and **3a–d** respectively. The reaction conditions and yields are summarized in Table 4, and spectroscopic and analytical data for the compounds are given in Tables 5 and 6. For the biological tests, each compound was re-purified on semipreparative HPLC with acetonitrile as the eluent. The acetonitrile was removed under reduced pressure and the product was recrystallized from a hexane–CH_2Cl_2 solution.

Table 4 Amount of reagents used, products and yields

Reaction	Zinc	$TiCl_4$	Ferrocenyl ketone	Benzophenone	Reaction time	Product	Yield
1	1.96 g (30 mmol)	3.79 g, 2.2 mL (20 mmol)	Benzyl ferrocenyl ketone 1.52 g (5 mmol)	4-Hydroxybenzophenone 0.99 g (5 mmol)	Overnight	**2c**	1.04 g (44%)
2	1.96 g (30 mmol)	3.79 g, 2.2 mL (20 mmol)	Phenyl ferrocenyl ketone 1.45 g (5 mmol)	4-Hydroxybenzophenone 0.99 g (5 mmol)	4 h	**2d**	1.19 g (52%)
3	1.96 g (30 mmol)	3.79 g, 2.2 mL (20 mmol)	4-Methoxyphenyl ferrocenyl ketone 1.60 g (5 mmol)	4-Hydroxybenzophenone 0.99 g (5 mmol)	Overnight	**2e**	0.88 g (36%)
4	7.84 g (120 mmol)	15.16 g, 8.8 mL (80 mmol)	Ethyl ferrocenyl ketone 4.84 g (20 mmol)	3,4-Dihydroxybenzophenone 4.28 g (20 mmol)	2 h	**3a**	5.52 g (65%)
5	1.96 g (30 mmol)	3.79 g, 2.2 mL (20 mmol)	[3]Ferrocenophan-1-one 1.20 g (5 mmol)	3,4-Dihydroxybenzophenone 1.07 g (5 mmol)	4 h	**3b**	0.99 g (47%)
6	3.92 g (60 mmol)	7.58 g, 4.4 mL (40 mmol)	Benzyl ferrocenyl ketone 3.04 g (10 mmol)	3,4-Dihydroxybenzophenone 2.14 g (10 mmol)	Overnight	**3c**	1.29 g (27%)
7	2.94 g (45 mmol)	11.37 g, 3.3 mL (30 mmol)	Phenyl ferrocenyl ketone 2.17 g (7.5 mmol)	3,4-Dihydroxybenzophenone 1.61 g (7.5 mmol)	4 h	**3d**	1.47 g (42%)

3.3 Acetylation of 3a

NaH (0.34 g, 8.50 mmol, 60% in oil) was added to a solution of **3a** (1.50 g, 3.53 mmol) dissolved in dry THF (60 mL). Acetyl chloride (0.55 mL, 7.80 mmol) was added and the mixture was stirred overnight at ambient temperature, after which 2 mL of ethanol was added.

After stirring for 10 min the solution was poured into water and extracted with CH_2Cl_2. The combined organic layers were dried on $MgSO_4$, filtered and the solvent was removed under reduced pressure. Chromatographic separation on a silica gel column with hexane–CH_2Cl_2 as the eluent afforded 4 (0.64 g, 36%) as well as a mixture of **5** and **6** (0.51 g, 31%), respectively. For the biological tests, **4** was re-purified on semi-preparative HPLC with acetonitrile as the eluent. The acetonitrile was removed under reduced pressure and the product was recrystallized from a hexane–CH_2Cl_2 solution.

3.4 Oxidation reactions

3.4.1 Oxidation of 2c. Silver oxide (0.10 g, 0.4 mmol) was added to a solution of **2c** (0.10 g, 0.2 mmol) in 8 mL of acetone and the mixture was stirred at room temperature in the dark. At hourly intervals a sample was withdrawn, filtered and the solvent removed under reduced pressure, after which NMR spectroscopic analysis was carried out. Quantitative formation of **7** was observed after 2 h. **7**: IR(CH_2Cl_2) ν(CO) (cm^{-1}): 1709. Other spectroscopic and analytical data are given in Tables 5 and 6.

3.4.2 Oxidation of 3a–d. In a typical reaction, silver oxide (0.12 g, 0.5 mmol) was added to a solution of the ferrocenyl catechol (0.1 mmol) in 3 mL $(CD_3)_2CO$ and the mixture was stirred at room temperature. Quantitative formation of **8b–d** was observed after 20 min; **8a** after 1 h. IR(CH_2Cl_2) ν(CO) (cm^{-1}): 1647 (**8a**); 1658 (**8b**); 1651 (**8c**); 1650 (**8d**). NMR data are given in Table 5.

Table 5 NMR data for compounds **2c–e** and **3–8**

Compound	^{1}H NMR, δ (ppm)	^{13}C NMR, δ/ppm
2c	7.16–7.08 (m, 10H, 2C$_6H_5$), 6.96 (d, J = 7.9 Hz, 2H, C$_6H_4$), 6.64 (d, J = 7.9 Hz, 2H, C$_6H_4$), 4.68 and 4.64 (s, br, 1H, OH), 4.12 and 4.10 (s, 5H, C$_5H_5$), 3.97 and 3.94 (t, J = 1.9 Hz, 2H, C$_5H_4$), 3.91 and 3.87 (s, 2H, CH_2), 3.80 and 3.74 (t, J = 1.9 Hz, 2H, C$_5H_4$) [*isomers present in 1 : 1 ratio*]	153.3, 153.2, 143.7, 143.4, 140.9, 139.4, 136.1, 135.9, 132.5, 132.1 (C^{quat}), 130.6, 130.0, 129.2, 128.7, 127.5, 127.4, 127.3, 126.9, 125.6, 125.5, 124.8, 114.3 (C_6H$_5$, C_6H$_4$), 87.5, 87.2 (Fc^{ipso}), 69.4, 69.3 (C_5H$_4$), 68.8, 68.7 (C_5H$_5$), 67.6, 67.5 (C_5H$_4$), 40.0, 39.9 (CH$_2$)
2d	7.37–7.07 (m, 10H, 2C$_6H_5$), 6.90 and 6.82 (d, J = 7.3 Hz, 2H, C$_6H_4$), 6.69 and 6.37 (d, J = 7.3 Hz, 2H, C$_6H_4$), 4.66 (s, br, 1H, OH), 4.35 and 4.33 (t, J = 1.9 Hz, 2H, C$_5H_4$), 4.30 (s, 5H, C$_5H_5$), 4.19 and 4.13 (t, J = 1.9 Hz, 2H, C$_5H_4$)	145.2, 145.0, 144.3, 144.1, 140.0, 139.3, 138.5, 138.4 (C^{quat}), 133.4, 133.1, 132.0, 131.7, 130.5, 129.3, 129.2, 128.8, 128.2, 127.5, 117.5, 116.2 (C_6H$_5$, C_6H$_4$), 86.8, 85.9 (Fc^{ipso}), 72.2, 72.0 (C_5H$_4$), 71.9, 71.8

	[*isomers present in 1 : 1 ratio*]	(C_5H_5), 71.0, 70.9 (C_5H_4)
2e	7.35–7.09 (m, 5H, C_6H_5), 6.90 (d, J = 8.9 Hz, 2H, C_6H_4), 6.87 (d, J = 8.9 Hz, 2H, C_6H_4), 6.79 (d, J = 8.5 Hz, 2H, C_6H_4), 6.40 (d, J = 8.5 Hz, 2H, C_6H_4), 4.40 (s, br, 1H, O*H*), 4.07 (s, 5H, C_5H_5), 4.01 (t, J = 1.9 Hz, 2H, C_5H_4), 3.98 (t, J = 1.9 Hz, 2H, C_5H_4), 3.70 (s, 3H, OCH_3) [*major isomer*] 7.35–7.09 (m, 5H, C_6H_5), 6.93 (d, J = 8.7 Hz, 2H, C_6H_4), 6.75 (d, J = 8.7 Hz, 2H, C_6H_4), 6.70 (d, J = 8.9 Hz, 2H, C_6H_4), 6.68 (d, J = 8.9 Hz, 2H, C_6H_4), 4.68 (s, br, 1H, O*H*), 4.08 (s, 5H, C_5H_5), 3.73 (s, 3H, OCH_3), 3.51 (t, J = 1.9 Hz, 2H, C_5H_4), 3.43 (t, J = 1.9 Hz, 2H, C_5H_4) [*minor isomer*]	157.9, 154.4, 153.1, 144.5, 138.7, 138.6, 136.9, 134.8, 134.7 (C^{quat}), 132.2, 131.4, 131.1, 130.1, 129.8, 128.6, 127.3, 126.7, 125.4, 115.5, 114.3, 112.8, 112.7 (C_6H_5, C_6H_4), 86.4 (Fc^{ipso}), 70.0, 69.9 (C_5H_4), 69.3 (C_5H_5), 68.4, 68.3 (C_5H_4), 55.1 (OCH_3)
3a[a]	7.35–7.04 (m, 5H, C_6H_5), 6.84 (d, J = 8.2 Hz, 1H, C_6H_3), 6.70 (d, J = 2.0, 1H, C_6H_3), 6.60 (dd, J = 8.2 and 2.0 Hz, 1H, C_6H_3), 4.11 (s, 5H, C_5H_5), 4.04 (t, J = 1.9 Hz, 2H, C_5H_4), 3.84 (t, J = 1.9 Hz, 2H, C_5H_4), 2.65 (q, J = 7.5 Hz, 2H, CH_2), 1.05 (t, J = 7.5 Hz, 3H, CH_3) [*major isomer*] 7.35–7.04 (m, 5H, C_6H_5), 6.71 (d, J = 8.0 Hz, 1H, C_6H_3), 6.57 (d, J = 2.0, 1H, C_6H_3), 6.43 (dd, J = 8.0 and 2.0 Hz, 1H, C_6H_3), 4.12 (s, 5H, C_5H_5), 4.07 (t, J = 1.9 Hz, 2H, C_5H_4), 3.96 (t, J = 1.9 Hz, 2H, C_5H_4), 2.55 (q, J = 7.5 Hz, 2H, CH_2), 1.03 (t, J = 7.5 Hz, 3H, CH_3) [*minor isomer*] **3a** partially decomposed within 6 months. After purification by chromatography, the ratio between the two isomers evolved from 1 : 1 to 78 : 12.	144.8, 144.6, 143.1, 143.3, 142.1, 142.0 (C^{quat}), 129.8, 129.3, 128.2, 128.1, 126.1, 122.8, 122.6, 122.1 (C_6H_5, C_6H_3), 86.6, 85.7 (Fc^{ipso}), 69.3 (C_5H_4), 69.2 (C_5H_5), 68.1 (C_5H_4), 27.9 (CH_2), 15.6, 15.5 (CH_3)
3b[a]	7.63 (s, 1H, O*H*), 7.57 (s, 1H, O*H*), 7.38–7.22 (m, 5H, C_6H_5), 6.53 (d, ^3J = 8.1 Hz, 1H, C_6H_3), 6.51 (d, ^4J = 2.1 Hz, 1H, C_6H_3), 6.39 (dd, ^3J = 8.1 Hz, ^4J = 2.1 Hz, 1H, C_6H_3), 4.26 (s, 2H, C_5H_4), 4.04 (s, 2H, C_5H_4), 4.00 (s, 2H, C_5H_4), 3.94 (s, 2H, C_5H_4), 2.61 (m, 2H, CH_2), 2.30 (m, 2H, CH_2) [*major isomer*]	143.8, 142.2, 142.1, 136.5, 134.1, 133.9 (C^{quat}), 129.4, 128.3, 126.8, 124.0, 117.9, 114.5 (C_6H_5, C_6H_3), 87.1 (Fc^{ipso}), 70.6, 70.5, 69.4, 68.9 (C_5H_4), 40.9, 28.8 (CH_2)

	7.86 (s, 1H, O*H*), 7.84 (s, 1H, O*H*), 7.06–7.01 (m, 5H, C_6H_5), 6.82 (d, ^3J = 8.1 Hz, 1H, C_6H_3), 6.70 (d, ^4J = 2.1 Hz, 1H, C_6H_3), 6.62 (dd, ^3J = 8.1 Hz, ^4J = 2.1 Hz, 1H, C_6H_3), 4.24 (s, 2H, C_5H_4), 4.02 (s, 2H, C_5H_4), 3.97 (s, 2H, C_5H_4), 3.96 (s, 2H, C_5H_4), 2.75 (m, 2H, CH_2), 2.34 (m, 2H, CH_2) [*minor isomer*] **3b** partially decomposed within 6 months. After purification by chromatography, the ratio between the two isomers became 84 : 16.	
3c[a]	7.79 (s, 2H, O*H*), 7.35–7.11 (m, 10H, $2C_6H_5$), 6.74 (d, *J* = 8.0 Hz, 1H, C_6H_3), 6.66 (d, *J* = 2.0 Hz, 1H, C_6H_3), 5.63 (dd, *J* = 8.0 and 2.0 Hz, 1H, C_6H_3), 4.15 (s, 5H, C_5H_5), 4.13 (s, 2H, CH_2), 3.99 (t, *J* = 2.0 Hz, 2H, C_5H_4), 3.82 (t, *J* = 2.0 Hz, 2H, C_5H_4) [*major isomer*] 7.79 (s, 2H, O*H*), 7.35–7.11 (m, 10H, $2C_6H_5$), 6.75 (d, *J* = 8.5 Hz, 1H, C_6H_3), 6.74 (d, *J* = 2.0 Hz, 1H, C_6H_3), 6.65 (dd, *J* = 8.5 and 2.0 Hz, 1H, C_6H_3), 4.16 (s, 5H, C_5H_5), 4.02 (s, 2H, CH_2), 3.94 (t, *J* = 2.0 Hz, 2H, C_5H_4), 3.69 (t, *J* = 2.0 Hz, 2H, C_5H_4) [*minor isomer*] **3c** partially decomposed within 6 months. After purification by chromatography, the ratio between the two isomers became 60 : 40.	146.0, 145.8, 145.7, 144.9, 144.7, 142.9, 142.8, 141.3, 141.2, 137.4, 137.2, 133.7, 133.4 (C^{quat}), 130.7, 130.2, 129.2, 129.0, 128.7, 128.6, 127.2, 127.1, 126.4, 122.3, 122.0, 117.8, 117.5, 116.1, 116.0 (C6H5, C_6H_3), 87.8 (Fc^{ipso}), 70.7, 70.6 (C_5H_4), 70.0 (C_5H_5), 68.6 (C_5H_4), 41.3, 41.1 (CH_2)
3d[a]	7.43–6.43 (m, 13H, $2C_6H_5$ + C_6H_3), 4.15 (s, 5H, C_5H_5), 4.06 (t, *J* = 1.9 Hz, 2H, C_5H_4), 3.54 (t, *J* = 1.9 Hz, 2H, C_5H_4) [*major isomer*] 7.43–6.43 (m, 13H, $2C_6H_5$ + C_6H_3), 4.12 (s, 5H, C_5H_5), 4.01 (t, J = 1.9 Hz, 2H, C_5H_4), 3.39 (t, *J* = 1.9 Hz, 2H, C_5H_4) [*major isomer*] **3d** partially decomposed within 6 months. After purification by chromatography, the ratio between the two isomers became 55 : 45	145.0, 144.9, 142.4, 138.7, 135.1, 134.7, 132.9 (C^{quat}), 131.2, 130.1, 129.8, 128.8, 127.6, 127.4 (C_6H_5, C_6H_3), 87.7(Fc^{ipso}), 70.0 (C_5H_4), 69.5 (C_5H_5), 68.6 (C_5H_4)
4	7.28–6.80 (m, 8H, C_6H_5 + C_6H_3), 4.06 and 4.04 (s, 5H, C_5H_5), 4.02 and 4.01 (t, *J* = 1.9 Hz, 2H, C_5H_4), 3.90 and 3.81 (t, *J* = 1.9 Hz, 2H, C_5H_4), 2.51 and 2.45 (q, *J* = 7.3 Hz, 2H, CH_2), 2.16 (s, 3H, $COCH_3$), 2.13 (s, 3H, $COCH_3$), 0.98 and 0.92 (t, *J* = 7.3 Hz, 3H, CH_3)	168.2, 168.1 ($COCH_3$), 143.9, 143.7, 143.1, 142.9, 141.7, 140.4, 138.9, 138.7, 136.1 (C^{quat}), 130.0, 129.5, 128.4, 128.3, 128.2, 127.5, 126.5, 124.8, 124.3, 123.1, 122.9 (C_6H_5, C_6H_3), 86.4 (Fc^{ipso}), 69.6, 69.5 (C_5H_4), 69.4, 69.3 (C_5H_5), 68.7, 68.4

	[*isomers present in 1 : 1 ratio*]	(C_5H_4), 28.2, 27.9 (CH_2), 20.7, 20.6 ($COCH_3$), 15.5, 15.4 (CH_3)
5/6	7.25–6.48 (m, 16H, C_6H_5 + C_6H_3), 5.19 and 5.14 (s, 1H, O*H*), 5.03 and 4.93 (s, 1H, O*H*), 4.05 (s, 5H, C_5H_5), 4.03 (s, 5H, C_5H_5), 4.02 and 3.99 (t, *J* = 1.9 Hz, 4H, C_5H_4), 3.88 and 3.79 (t, *J* = 1.9 Hz, 4H, C_5H_4), 2.49 (m, 4H, CH_2), 2.29 and 2.28 (s, 3H, $COCH_3$), 2.26 and 2.22 (s, 3H, $COCH_3$), 0.96 (m, 6H, CH_3)	171.0 ($COCH_3$), 148.4, 147.3, 147.2, 145.9, 145.7, 145.4, 145.3, 145.0, 143.8, 140.2, 140.0, 139.5, 139.1, 138.6, 138.3 (C^{quat}), 131.5, 131.3, 130.9, 129.9, 129.7, 129.5, 128.5, 127.8, 127.6, 125.5, 124.9, 124.0, 123.8, 123.7, 123.3, 120.5, 119.2, 119.0 (C_6H_5, C_6H_3), 88.2, 88.1, 87.8, 87.7 (Fc^{ipso}), 70.9, 70.7 (C_5H_5), 69.9, 69.8, 69.7, 69.6 (C_5H_4), 29.5, 29.4 (CH_2), 22.5 ($COCH_3$), 17.2, 17.0 (CH_3)
7[a]	7.67–7.41 (m, 10H, C_6H_5), 7.25–7.17 (m, 3H, C*H*, quinone ring), 6.36 (m, 1H, quinone ring), 6.24 (m, 1H, C*H*, vinyl), 4.44 (m, 1H, C_5H_4), 4.37 (m, 1H, C_5H_4), 4.28 (m, 1H, C_5H_4), 4.23 (m, 1H, C_5H_4), 4.00 (s, 5H, C_5H_5)	187.2 (*C*=O), 157.3 (C^{quat}), 139.0 (C_6H_4, C_6H_5), 138.7 (C^{quat}), 137.8 (C_6H_4, C_6H_5), 137.4, 135.9 (C^{quat}), 131.3, 130.2 (C_6H_4, C_6H_5), 130.1 (C^{quat}), 129.4, 128.9, 128.8, 128.6, 128.5, 128.3, 127.5 (C_6H_4, C_6H_5), 87.8 (Fc^{ipso}), 69.7 (C_5H_5), 69.1, 69.0, 68.0, 66.6 (C_5H_4)
8a[a]	7.49–7.33 (m, 5H, C_6H_5), 6.64 (dd, *J* = 10.2 and 2.2 Hz, 1H, C_6H_3), 6.11 (dd, *J* = 10.2 and 0.6 Hz, 1H, C_6H_3), 5.83 (dd, *J* = 2.2 and 0.6 Hz, 1H, C_6H_3), 4.58 (t, *J* = 1.8 Hz, 2H, C_5H_4), 4.53 (t, *J* = 1.8 Hz, 2H, C_5H_4), 4.28 (s, 5H, C_5H_5), 2.74 (q, *J* = 7.5 Hz, 2H, CH_2), 0.95 (t, *J* = 7.5 Hz, 3H, CH_3) [*major isomer*] 7.49–7.33 (m, 5H, C_6H_5), 6.95 (dd, *J* = 10.1 and 2.2 Hz, 1H, C_6H_3), 6.39 (dd, *J* = 2.2 and 0.6 Hz, 1H, C_6H_3), 6.32 (dd, *J* = 10.1 and 0.6 Hz, 1H, C_6H_3), 4.18 (t, *J* = 1.9 Hz, 2H, C_5H_4), 4.17 (s, 5H, C_5H_5), 3.91 (t, *J* = 1.9 Hz, 2H, C_5H_4), 2.92 (q, *J* = 7.5 Hz, 2H, CH_2), 1.24 (t, *J* = 7.5 Hz, 3H, CH_3) [*minor isomer*] [*isomers present in 81 : 19 ratio*]	182.0, 179.8 (*C*=O), 156.5, 150.5 (C^{quat}), 144.9 (C_6H_5, C_6H_3), 142.8, 136.3 (C^{quat}), 130.9, 129.8, 129.7, 128.3, 128.0 (C_6H_5, C_6H_3), 89.0 (Fc^{ipso}), 71.6, 71.3 (C_5H_4), 70.5 (C_5H_5), 44.7 (CH_2), 15.7 (CH_3)
8b[a]	7.49–7.37 (m, 5H, C_6H_5), 6.95 (dd, *J* = 10.2 and 2.2 Hz, 1H, C_6H_3), 6.03 (dd, *J* = 10.2 and 0.7 Hz, 1H, C_6H_3), 5.88 (dd, *J* = 2.2 and 0.7 Hz, 1H, C_6H_3), 4.49 (t, *J* = 1.8 Hz, 2H, C_5H_4), 4.46 (t, *J* = 1.8 Hz, 2H, C_5H_4), 4.25 (t, *J* = 1.8 Hz, 2H, C_5H_4), 3.98 (t, *J* = 1.8 Hz, 2H, C_5H_4), 2.74 (m,	181.6, 180.2 (*C*=O), 154.5, 145.5, 143.4, 142.8, 141.3 (C^{quat}), 131.5, 130.2, 129.6, 128.7, 127.7 (C_6H_5, C_6H_3), 88.2, 83.3 (Fc^{ipso}), 71.7, 71.5, 70.1, 69.2 (C_5H_4), 41.8, 29.7 (CH_2)

	2H, CH_2), 2.45 (m, 2H, CH_2) [*major isomer*] 7.49–7.37 (m, 5H, C_6H_5), 6.72 (dd, *J* = 10.1 and 2.2 Hz, 1H, C_6H_3), 6.52 (dd, *J* = 2.2 and 0.8 Hz, 1H, C_6H_3), 6.28 (dd, *J* = 10.1 and 0.8 Hz, 1H, C_6H_3), 4.37 (t, *J* = 1.8 Hz, 2H, C_5H_4), 4.07 (t, *J* = 1.8 Hz, 2H, C_5H_4), 4.04 (t, *J* = 1.8 Hz, 2H, C_5H_4), 3.94 (t, *J* = 1.8 Hz, 2H, C_5H_4), 3.05 (m, 2H, CH_2), 2.51 (m, 2H, CH_2) [*minor isomer*] [*isomers present in 84 : 16 ratio*]	
8c[a]	7.38–7.11 (m, 10H, 2C_6H_5), 6.72 (dd, *J* = 10.2 and 2.2 Hz, 1H, C_6H_3), 6.14 (dd, *J* = 10.2 and 0.7 Hz, 1H, C_6H_3), 5.92 (dd, *J* = 2.2 and 0.7 Hz, 1H, C_6H_3), 4.45 (broad singlet, 4H, tentatively attributed to C_5H_4), 4.35 (s, 5H, C_5H_5), 4.13 (s, 2H, CH_2) [*major isomer*] 7.38–7.11 (m, 10H, 2C_6H_5), 6.64 (dd, *J* = 10.1 and 2.1 Hz, 1H, C_6H_3), 6.45 (dd, *J* = 2.1 and 0.6 Hz, 1H, C_6H_3), 6.06 (dd, *J* = 10.1 and 0.6 Hz, 1H, C_6H_3), 4.24 (s, 5H, C_5H_5), 4.15 (t, *J* = 1.9 Hz, 2H, C_5H_4), 3.88 (t, *J* = 1.9 Hz, 2H, C_5H_4), the signal for CH_2Ph could not be clearly identified [*minor isomer*] [*isomers present in 65 : 35 ratio*]	The instability of this compound precluded characterization by ^{13}C NMR.
8d[a]	7.69–7.10 (m, 10H, 2C_6H_5), 6.83 (dd, *J* = 10.2 and 2.2 Hz, 1H, C_6H_3), 5.95 (dd, *J* = 2.2 and 0.6 Hz, 1H, C_6H_3), 5.88 (dd, *J* = 2.2 and 0.6 Hz, 1H, C_6H_3), 4.25 (s, 5H, C_5H_5), 4.24 (t, *J* = 2.0 Hz, 2H, C_5H_4), 3.51 (t, *J* = 2.0 Hz, 2H, C_5H_4) [*major isomer*] 7.69–7.10 (m, 10H, 2C_6H_5), 6.82 (dd, *J* = 10.1 and 2.2 Hz, 1H, C_6H_3), 6.29 (dd, *J* = 10.1 and 0.7 Hz, 1H, C_6H_3), 6.23 (dd, *J* = 2.2 and 0.7 Hz, 1H, C_6H_3), 4.48 (t, *J* = 1.9 Hz, 2H, C_5H_4), 4.30 (t, *J* = 1.9 Hz, 2H, C_5H_4), 4.28 (s, 5H, C_5H_5) [*minor isomer*] [*isomers present in 73 : 27 ratio*]	181.4, 180.0 (*C*=O), 155.3, 147.2, 142.9, 142.0, 136.4 (C^{quat}), 131.7, 131.6, 131.1, 130.0, 128.9, 128.7, 127.7 (C_6H_5, C_6H_3), 84.7 (Fc^{ipso}), 70.6 (C_5H_5), 71.6, 70.7 (C_5H_4)

[a] In CD_3COCD_3.

Table 6 MS and analytical data for compounds **2c–e** and **3–7**

	MS, *m/z*	HRMS, *m/z*	
Compound	Found (calculated for M^+)	Found (calculated for M^+)	Elemental analysis: found (calculated) %
2c	470 (470)	$C_{31}H_{26}FeO$: 470.1327 (470.1333)	$C_{31}H_{26}FeO·0.25H_2O$: C, 78.57 (78.40); H, 5.68 (5.62)[a]
2d	456 (456)	$C_{30}H_{24}FeO$: 456.1171 (456.1177)	$C_{30}H_{24}FeO·0.5H_2O$: C, 77.39 (77.43); H, 5.43 (5.41)[a]
2e	487 [MH^+] (486)	$C_{31}H_{26}FeO_2$: 486.1277 (486.1282)	$C_{31}H_{26}FeO_2·H_2O$: C, 74.09(73.82); H, 5.89 (5.60)[a]
3a	424 (424)	$C_{26}H_{24}FeO_2$: 424.1120 (424.1126)	$C_{26}H_{24}FeO_2$: C, 73.19 (73.59); H, 5.79 (5.70)
3b	422 (422)	$C_{26}H_{22}FeO_2$: 422.0958 (422.0969)	$C_{26}H_{22}FeO_2·0.25H_2O$: C, 72.87 (73.12); H, 5.35 (5.31)[a]
3c	486 (486)	$C_{31}H_{26}FeO_2$: 486.1282 (486.1282)	$C_{31}H_{26}FeO_2·0.5H_2O$: C, 75.18 (75.16); H, 5.62 (5.49)[a]
3d	472 (472)	$C_{30}H_{24}FeO_2$: 472.1125 (472.1126)	$C_{30}H_{24}FeO_2·0.25H_2O$: C, 75.45 (75.56); H, 5.52 (5.18)[a]
4	508 (508)	$C_{30}H_{28}FeO_4$: 508.1332 (508.1337)	$C_{30}H_{28}FeO_4·0.5H_2O$: C, 69.61 (69.94); H, 5.61 (5.65)[a]
5/6	466 (466)	$C_{28}H_{26}FeO_3$: 466.1221 (466.1231)	$C_{28}H_{26}FeO_3·0.5C_6H_{14}$: C, 72.94 (73.09); H, 6.59 (6.53)[b]
7	468 (468)	$C_{31}H_{24}FeO$: 468.1171 (468.1177)	$C_{31}H_{24}FeO·2H_2O$: C, 74.11 (73.82); H, 5.91 (5.60)[a]

[a] Presence of water in the analytical sample was verified by ^{1}H NMR spectroscopy. [b] Presence of hexane in the analytical sample was verified by ^{1}H NMR spectroscopy.

Table 7 Crystal data for *E*-**2c**, *Z*-**2d**, *Z*-**2e** and *Z*-**4**

Compound	*E*-**2c**	*Z*-**2d**	*Z*-**2e**	*Z*-**4**
Formula	$C_{31}H_{26}FeO$	$C_{30}H_{24}FeO$	$C_{31}H_{26}FeO_2$	$C_{30}H_{28}FeO_4$
F_w	470.37	456.34	486.37	508.37
Crystal system	Monoclinic	Monoclinic	Triclinic	Monoclinic
Space group	$P2_1/c$	$P2_1/n$	$P\bar{1}$	$P2_1/c$
Unit cell dimensions				
a (Å)	14.950(2)	9.7144(4)	9.4498(2)	12.1301(4)
b (Å)	9.9214(13)	12.9617(5)	11.5084(2)	17.0739(5)
c (Å)	15.579(2)	17.6055(7)	12.0193(2)	12.8231(3)
α (°)	90	90	71.0240(10)	90
β (°)	98.413(7)	95.1240(10)	81.4350(10)	112.2770(10)
γ (°)	90	90	66.1580(10)	90
Volume (Å^3)	2285.8(5)	2207.95(15)	1130.37(4)	2457.55(12)
Z	4	4	2	4
ρ_c (mg m^{-3})	1.367	1.373	1.429	1.374
μ (Mo Kα) (mm^{-1})	0.682	0.703	0.695	0.648
F(000)	984	952	508	1064

Crystal size (mm^3)	0.40 × 0.20 × 0.10	0.33 × 0.11 × 0.11	0.40 × 0.40 × 0.06	0.40 × 0.31 × 0.22
θ range (°)	2.44 to 30.51	2.31 to 26.36	1.79 to 31.07	2.09 to 26.37
Reflections collected	49 324	26 025	19 666	56 571
Independent reflections (R_{int})	4676 (0.0650)	4461 (0.0530)	4609 (0.0309)	5015 (0.0543)
Completeness % (to θ, deg)	99.9 (26.37)	99.0 (26.36)	99.8 (26.37)	99.8 (26.37)
Transmission range	0.9350–0.7722	0.9266–0.8011	0.9595–0.7685	0.8705–0.7815
Data/restraints/parameters	4676/6/308	4461/0/303	4609/1/321	5015/0/428
Goodness-of-fit on F^2	1.220	1.166	1.195	1.168
Final R indices [$I > 2\sigma(I)$]	R_1 = 0.0441, wR_2 = 0.1159	R_1 = 0.0464, wR_2 = 0.1516	R_1 = 0.0322, wR_2 = 0.0924	R_1 = 0.0331, wR_2 = 0.1036
R indices (all data)	R_1 = 0.0773, wR_2 = 0.1543	R_1 = 0.0573, wR_2 = 0.1676	R_1 = 0.0410, wR_2 = 0.1180	R_1 = 0.0422, wR_2 = 0.1252
Largest diff. peak and hole (e $Å^{-3}$)	0.564 and −0.617	0.484 and −0.553	0.426 and −0.482	0.611 and −0.661

3.5 Electrochemistry

Cyclic voltammograms (CVs) were obtained using a three electrode cell with a 0.5 mm Pt working electrode, stainless steel rod counter electrode, and Ag/AgCl ethanol reference electrode, with an μ-Autolab 3 potentiostat driven by GPES software (General Purpose Electrochemical System, Version 4.8, EcoChemie B.V., Utrecht, the Netherlands). Solutions consisted of 10 mL CH_2Cl_2, approximately 1 mM analyte, and 0.1 M Bu_4NPF_6 supporting electrolyte. After obtaining the cyclic voltammograms in CH_2Cl_2, two drops of lutidine were added to the cell and data was obtained.

Preparative electrolyses were carried out in acetonitrile under argon atmosphere in a 2 × 5 cm^3 two-compartment cell with a n° 4 porosity sintered glass separator. The anodic compartment was equipped with a platinum grid anode (1 cm^2) and a SCE reference electrode, the cathodic compartment being fitted with a 1 cm^2 area platinum grid cathode. The compartments were filled with 5 mL of acetonitrile containing Bu_4NBF_4 (0.2 mol L^{-1}). Compounds **3a** or **3c** were introduced in the anodic compartment and 9-fluorenone (0.25 mmol) was introduced in the cathodic compartment in order to provide a reproducible and easy auxiliary cathodic reaction. The electrolyses were stopped until a charge of 2 Faraday per mole was passed. The electrolyses were monitored by cyclic voltammetry (CV) at a 0.5 mm Pt electrode. Electrolyses and CVs were recorded on a PAR 2273 potentiostat.

3.6 Biochemistry

The human cell MDA-MB-231 (breast adenocarcinoma) purchased from ATCC was grown in RPMI medium supplemented with 10% fetal calf serum, in the presence of penicillin, streptomycin and fungizone in 75 cm^3 flasks under 5% CO_2. For cytotoxicity determinations, cells were plated in 96-well tissue culture microplates in 200 μL complete medium and treated 24 h later with compounds dissolved in DMSO using a Biomek 3000 (Beckman-Coulter). Controls received the same volume of DMSO (1% final volume). After 72 h exposure, MTS reagent (Promega) was added and incubated for 3 h at 37 °C: the absorbance was monitored at 490 nm and results expressed as the inhibition of cell proliferation calculated as the ratio {[1 − (OD490 treated/OD490 control)] × 100} in triplicate experiments. For IC_{50} experiments performed in duplicate, compounds were added in the range 0.5 nM^{-10} μM in a fixed volume of DMSO.

3.7 X-ray crystal structure determinations

Crystals were mounted on quartz fibers. X-ray data were collected using a Bruker AXS APEX system, using Mo Kα radiation, with the SMART suite of programs.[35] Data were processed and corrected for Lorentz and polarization effects with SAINT,[36] and for absorption effects with SADABS.[37] Structural solution and refinement were carried out with the SHELXTL suite of programs.[38] Crystal and refinement data are summarized in Table 7.

The structures were solved by direct methods to locate the heavy atoms, followed by difference maps to complete the structure. Organic hydrogen atoms were placed in calculated positions and refined with a riding model; hydroxyl hydrogen atoms were either located or placed in calculated positions and refined with appropriate distance restraints. All non-hydrogen atoms were given anisotropic displacement parameters in the final model.

There was disorder of the hydroxyl group in *E*-**2c** and *Z*-**2e** over two aromatic rings in each case. These were refined with appropriate restraints and on their occupancies which were constrained to sum to unity.

Conclusion

In our ongoing investigations on the anti-proliferative activity of conjugated phenylferrocene systems, we have synthesized a series of ferrocenyl catechols *via* the McMurry coupling reaction and tested their anti-proliferative effects on hormone-independent breast cancer cell lines. These ferrocenyl catechols **3** were found to have equivalent or higher efficacy than their

phenolic analogues **2**, in contrast to previous reports on the phenol and catechol metabolites of tamoxifen and toremifen. The ability to form oxidation products, either QMs or OQs is closely related to their activity in the *in vitro* assays. Consistent with our earlier investigations, the catechol bearing the [3]ferrocenophane motif, *viz*. **3b**, displays greater anti-proliferative potency than its ferrocenyl analogue **2b**.

Interestingly, molecules that could theoretically form QM or OQs (**3a** and **3c**) seem to exclusively favor the OQ structure under chemical oxidation. We were surprised that, whatever the metabolites favored in the biological milieu, the anti-proliferative effects are quite similar. Further work will include metabolism studies using biologically relevant oxidants. The reaction of QM and OQ forms of these ferrocenyl phenol and catechol compounds with biologically relevant nucleophiles such as glutathione and deoxynucleosides are the subject of current investigations.

Acknowledgements

We thank Dr Li Yongxin for crystallographic assistance and Dr Thierry Cresteil for biochemical tests. Financial support was provided by the Agence Nationale de la Recherche (No. ANR-06-BLAN-0384-01, “FerVect”, postdoctoral fellowship for Y. L. K. T.) and COST (D39 WG001).

References

1 B. Fisher, J. Costantino, C. Redmond, R. Poisson, D. Bowman, J. Couture, N. V. Dimitrov, N. Wolmark, D. L. Wickerham, E. R. Fisher, R. Margolese, A. Robidocex, H. Shibotu, J. Terz, A. H. G. Paterson, H. L. Lickley and M. Ketner, *N. Engl. J. Med*., 1989, **320**, 479–484.

2 C. K. Osbourne, *N. Engl. J. Med*., 1998, **339**, 1609–1618.

3 G. N. Hortobagyi, *N. Engl. J. Med*., 1998, **339**, 974–984.

4 S. G. Nayfield, J. E. Karp, L. G. Ford, F. A. Dorr and B. S. Kramer, *J. Nat. Cancer Inst*., 1991, **23**, 1450–1459.

5 V. C. Jordan, *J. Med. Chem*., 2003, **46**, 883–908.

6 V. C. Jordan, *J. Med. Chem*., 2003, **46**, 1081–1108.

7 L. L. Smith and I. N. White, *Oncology*, 1998, **12**, 14–22.

8 M. A. Killackey, T. B. Hakes and V. K. Price, *Cancer Treat. Rep*., 1985, **69**, 237–238.

9 G. K. Poon, B. Walter, P. E. Lonning, M. N. Holton and R. McCague, *Drug Metab. Dispos*., 1995, **23**, 377–382.

10 X. Liu, E. Pisha, D. A. Tonetti, D. Yao, Y. Li, J. Yao, J. E. Burdette and J. L. Bolton, *Chem. Res. Toxicol*., 2003, **16**, 832–837.

11 S. S. Dehal and D. Kupfer, *Cancer Res*., 1995, **56**, 1283–1290.

12 S. Top, J. Tang, A. Vessières, D. Carrez, C. Provot and G. Jaouen, *Chem. Commun*., 1996, 955–956.

13 S. Top, A. Vessières, C. Cabestaing, I. Laios, G. Leclercq, C. Provot and G. Jaouen, *J. Organomet. Chem*., 2001, **637–639**, 500–506.

14 S. Top, A. Vessières, G. Leclercq, J. Quivy, J. Tang, J. Vaissermann, M. Huché and G. Jaouen, *Chem.–Eur. J*., 2003, **9**, 5223–5236.

15 G. Jaouen, S. Top, A. Vessières, G. Leclercq and M. J. McGlinchey, *Curr. Med. Chem*., 2004, **11**, 2505–2517.

16 A. Vessières, S. Top, W. Beck, E. A. Hillard and G. Jaouen, *Dalton Trans*., 2006, 529–541.

17 E. A. Hillard, P. Pigeon, A. Vessières, C. Amatore and G. Jaouen, *Dalton Trans*., 2007, 5073–5081.

18 E. A. Hillard, A. Vessières, F. Le Bideau, D. Plażuk, D. Spera, M. Huché and G. Jaouen, *ChemMedChem*, 2006, **1**, 551–559.

19 A. Valentini, F. Conforti, A. Crispini, A. D. Martino, R. Condello, C. Stellitano, G. Rotilio, M. Ghedini, G. Federici, S. Bernardini and D. Pucci, *J. Med. Chem*., 2009, **52**, 484–491.

20 E. A. Hillard, A. Vessières, L. Thouin, G. Jaouen and C. Amatore, *Angew. Chem., Int. Ed*., 2006, **45**, 285–290.

21 D. Hamels, P. M. Dansette, E. A. Hillard, S. Top, A. Vessières, G. Jaouen and D. Mansuy, *Angew. Chem., Int. Ed*., 2009, **48**, 9124–9126.

22 D. Plazuk, A. Vessières, E. A. Hillard, O. Buriez, E. Labbé, P. Pigeon, M.-A. Plamont, C. Amatore, J. Zakrzewski and G. Jaouen, *J. Med. Chem*., 2009, **52**, 4964–4967.

23 M. Gormen, D. Plazuk, P. Pigeon, E. A. Hillard, M.-A. Plamont, S. Top, A. Vessières and G. Jaouen, *Tetrahedron Lett*., 2010, **51**, 118–120.

24 M. Gormen, P. Pigeon, S. Top, A. Vessières, M.-A. Plamont, E. A. Hillard and G. Jaouen, *Med. Chem. Commun*., 2010, **1**, 149–151.

25 During the preparation of this manuscript, we discovered the article F. Zhao, C. Zhao and Z.-Q. Liu, *J. Biol. Inorg. Chem*, 2011, **16**, 1169– 1176. This article reports the synthesis of **2d**, **3a** and **3d** by similar methods as reported here.

26 Y. L. K. Tan, P. Pigeon, E. A. Hillard, S. Top, M.-A. Plamont, A. Vessières, M. J. McGlinchey, H. Müller-Bunz and G. Jaouen, *Dalton Trans*., 2009, 10871–10881.

27 P. Messina, E. Labbé, O. Buriez, E. A. Hillard, A. Vessières, D. Hamels, S. Top, G. Jaouen, Y. M. Frapart, D. Mansuy and C. Amatore, *Chem.– Eur. J*., 2012, DOI: 10.1002/chem.201103378.

28 A. Vessières, S. Top, P. Pigeon, L. Boubeker, D. Spera and G. Jaouen, *J. Med. Chem*., 2005, **48**, 3937–3940.

29 J. B. Heilmann, E. A. Hillard, M. A. Plamont, P. Pigeon, M. Bolte, G. Jaouen and A. Vessières, *J. Organomet. Chem*., 2008, **693**, 1716– 1722.

30 D. Yao, F. Zhang, L. Yu, Y. Yang, R. B. van Breemen and J. L. Bolton, *Chem. Res. Toxicol*., 2001, **14**, 1643–1653.

31 M. Gormen, P. Pigeon, S. Top, E. A. Hillard, M. Huché, C. G. Hartinger, F. de Montigny, M.-A. Plamont, A. Vessières and G. Jaouen, *ChemMedChem*, 2010, **5**, 2039–2050.

32 D. Enders, R. Peters, G. Raabe, J. Runsick and J. W. Bats, *Eur. J. Org. Chem*., 2000, 3399–3426.

33 A. C. Benyei, C. Glidewell, P. Lightfoot, B. J. L. Royles and D. M. Smith, *J. Organomet. Chem*., 1997, **539**, 177–186.

34 T. D. Turbitt and W. E. Watts, *J. Organomet. Chem*., 1972, **46**, 109–117.

35 *SMART, version 5.628*, Bruker Advanced Analytical X-ray Systems, Inc., Madison, WI, USA, 2001.

36 *SAINT+, version 6.22a*, Bruker Advanced Analytical X-ray Systems, Inc., Madison, WI, USA, 2001.

37 G. M. Sheldrick, *SADABS, Program for area detector adsorption correction*, Institute for Inorganic Chemistry, University of Göttingen, Germany, 1996.

38 *SHELXTL, version 5.1*, Bruker Advanced Analytical X-ray Systems, Inc., Madison, WI, USA, 1997.